Spectral convergence of the generalized Polynomial Chaos reduced model obtained from the uncertain linear Boltzmann equation

Gaël Poëtte

Spectral convergence of the generalized Polynomial Chaos reduced model obtained from the uncertain linear Boltzmann equation

Gaël Poëtte*

April 4, 2019

Abstract

In this paper, we consider the linear Boltzmann equation subject to uncertainties in the initial conditions and matter parameters (cross-sections/opacities). In order to solve the underlying uncertain systems, we rely on moment theory and the construction of hierarchical moment models in the framework of parametric polynomial approximations. Such model is commonly called a generalised Polynomial Chaos (gPC) reduced model. In this paper, we prove the spectral convergence of the hierarchy of reduced model parametered by P (polynomial order) obtained from the uncertain linear Boltzmann equation.

1 Introduction

In this paper, we are interested in the linear Boltzmann equation recalled below

$$\begin{cases} \partial_t u(\mathbf{x},t,\mathbf{v}) + \mathbf{v}\cdot\nabla_{\mathbf{x}} u(\mathbf{x},t,\mathbf{v}) = -v\sigma_t(\mathbf{x},t,\mathbf{v})u(\mathbf{x},t,\mathbf{v}) + \displaystyle\int v\sigma_s(\mathbf{x},t,\mathbf{v},\mathbf{v}')u(\mathbf{x},t,\mathbf{v}')\,\mathrm{d}\mathbf{v}', \\ u(\mathbf{x},0,\mathbf{v}) = u_0(\mathbf{x},\mathbf{v}). \end{cases} \tag{1}$$

It models the time-dependent problem of particle transport in a collisional media. We suppose transport to be driven by the linear Boltzmann equation (1) for particles having position $\mathbf{x}\in\mathcal{D}\subset\mathbb{R}^3$, velocity $\mathbf{v}\in\mathcal{V}\subset\mathbb{R}^3$, at time $t\in[0,T]\subset\mathbb{R}^+$ and where the quantity $u(\mathbf{x},t,\mathbf{v})\in\Omega\subset\mathbb{R}^+$ is the density of presence of the particles at $(\mathbf{x},t,\mathbf{v})$. In (1), we introduced the notation $|\mathbf{v}|=v$ to denote the norm of the velocity $\mathbf{v}$. Later on, we may also use $\omega=\frac{\mathbf{v}}{v}$, the unitary vector for the direction of the particles. Equation (1) must come with proper boundary conditions for wellposedness [33, 25] but we omit them for the sake of conciseness. In other words, the Cauchy problem (1) is valid in an infinite medium and regular solutions can be expected [25, 9, 38, 48]. The left hand side of (1) will be hinted at as the *streaming* counterpart of (1) whereas its right hand side will be called the *collisional* one. The above equation is linear and can be used to model the behaviour of particles interacting with a *background* media. The interaction of particles with matter is described through the macroscopic total interaction probability of particles with media $\sigma_t(\mathbf{x},t,\mathbf{v})$ and the scattering one $\sigma_s(\mathbf{x},t,\mathbf{v},\mathbf{v}')$. A solution of (1) is called a deterministic solution.

Let us assume that the initial condition and the cross-sections are uncertain. It means that we would like to solve (1) for many different values X of the initial condition and cross-sections. It is common to make the dependence with respect to X explicit so that

$$u_0 = u_0(x,X)\in\Omega \text{ and } \sigma_\alpha = \sigma_\alpha(\cdot,X) \text{ for } \alpha\in\{s,t\} \text{ and with } X\in\Theta\subset\mathbb{R}^Q. \tag{2}$$

*CEA, CESTA, DAM, F-33114 Le Barp, France

The variable $X \in \Theta$ characterizes what is called the uncertainty, where the set $\Theta = (\Theta, \mathcal{A}, \mathcal{P})$ is a probability space where Θ is the sample space, $\mathcal{A}$ is a σ-algebra and $\mathcal{P}$ a probability measure. We assume X comes with its probability measure $\mathrm{d}\mathcal{P}_X$. Note that without loss of generality in the following sections, we consider that X is a vector $X = (X_1, ..., X_Q)^t$ of Q independent random variables of probability measure $\mathrm{d}\mathcal{P}_X = \prod_{i=1}^{Q} \mathrm{d}\mathcal{P}_{X_i}$: in theory, it is always possible to come back to such framework[1]. Note also that $\mathrm{d}\mathcal{P}_X$ sums up to one, i.e. $\int \mathrm{d}\mathcal{P}_X = 1$. Furthermore, without loss of generality, X can be mapped into a vector of uniform random variables $\mathcal{U} = (\mathcal{U}_1, ..., \mathcal{U}_Q)$ on $[0,1]^Q$. As a consequence, wherever one is willing to integrate any function[2] $f \in L^1(\Theta)$ with respect to measure $\mathrm{d}\mathcal{P}_X$, one can perform the change of variable

$$\int f(X)\,\mathrm{d}\mathcal{P}_X = \int f(X(\mathcal{U}))\,\mathrm{d}\mathcal{P}_{\mathcal{U}} = \int f(X(u))\mathbf{1}_{[0,1]}(u)\,\mathrm{d}u. \tag{3}$$

As a consequence, it is not restrictive in the following to consider X is uniformly distributed as this is always true up to a change of variable.
In some sense if one solves (1) for all different initial condition and cross-sections that correspond to different X, then one exactly propagates the uncertainties. To fix the notations, system

$$\begin{cases} \partial_t u(\mathbf{x}, t, \mathbf{v}, X) + \mathbf{v} \cdot \nabla_{\mathbf{x}} u(\mathbf{x}, t, \mathbf{v}, X) = -v\sigma_t(\mathbf{x}, t, \mathbf{v}, X) u(\mathbf{x}, t, \mathbf{v}, X) \\ \qquad\qquad + \displaystyle\int v\sigma_s(\mathbf{x}, t, \mathbf{v}, \mathbf{v}', X) u(\mathbf{x}, t, \mathbf{v}', X)\,\mathrm{d}\mathbf{v}', \\ u(\mathbf{x}, 0, \mathbf{v}, X) = u_0(\mathbf{x}, \mathbf{v}, X), \end{cases} \tag{4}$$

for $\mathbf{x} \in \mathcal{D} \subset \mathbb{R}^3, \mathbf{v} \in \mathcal{V} \subset \mathbb{R}^3, t \in [0, T] \subset \mathbb{R}^+, X \in \Theta \subset \mathbb{R}^Q$ will be called a uncertain problem. One notices that different values of X correspond to different fully decoupled deterministic equations, so in principle there is no difficulty in solving such uncertain problems. The whole problem comes from the fact that exact propagation of uncertainties is very expensive from the computational point of view: equation (1) is often solved thanks to a Monte-Carlo scheme [33, 48, 38, 8, 1, 41, 15, 46]. This resolution method is known to be efficient for high $(3(\mathbf{x}) + 1(t) + 3(\mathbf{v}) = 7)$ dimensional problems but costly. This is emphasized, detailed and illustrated in [47]. In [47], a P-truncated gPC reduced model has been introduced in order to solve (4). It is solved thanks to a astute Monte-Carlo resolution of the gPC reduced model. Note that a similar approach has been developed for the Fokker-Planck equation in [11]. In [47], fast convergence has been practically observed with respect to the truncation order P. The aim of this paper is to explain this fast convergence and for this, in the following sections, we prove the spectral convergence of the $P-$truncated gPC based reduced models obtained from (4).

The paper is organized as follows. In section 2, we present the P-truncated gPC reduced model of interest here (and solved in [47]). In section 3, we prove the spectral convergence of the built reduced model. In section 4, we present few numerical results confirming the theoretical results of section 3. They are obtained with the resolution schemes presented in [47]. We finally conclude in section 5 with emphasis on the remaining open questions.

2 The gPC reduced model obtained from the uncertain linear Boltzmann equation (4)

The standard method to construct a gPC based reduced model is the following. We first define the set of k integrable uncertain functions

$$L^k_\Theta = \left\{ \text{measurable functions } X \mapsto f(X) \text{ such that } \int_\Theta |f(\xi)|^k\,\mathrm{d}\mathcal{P}_X(\xi) < \infty \right\}. \tag{5}$$

[1] At the cost of more or less tedious pretreatments leading to a controled approximation [51, 44, 49, 43] and decorrelation [35, 36].
[2] See (5) for the definition of $L^1(\Theta)$.

In particular, we focus on functions of $L^2(\Theta)$. Under very general conditions [17, 19], there exists a countable family of polynomials $(\phi_q)_{q\in\mathbb{N}}$ which are orthonormal with respect to the scalar product defined by $\mathrm{d}\mathcal{P}_X$. In other words, we have

$$\int_\Theta \phi_p(\xi)\phi_q(\xi)\,\mathrm{d}\mathcal{P}_X(\xi) = \int \phi_p\phi_q\,\mathrm{d}\mathcal{P}_X = \delta_{pq}, \forall (p,q)\in\mathbb{N}^2.$$

At fixed $t\in[0,T]\subset\mathbb{R}^+, \mathbf{x}\in\mathcal{D}\subset\mathbb{R}^3$ and $\mathbf{v}\in\mathcal{V}\subset\mathbb{R}^3$, it is natural to look for an approximation of the solution u in the subspace $(\phi_k)_{k\in\{0,\dots,P\}}$ generated by the first $P+1$ polynomials of $(\phi_k)_{k\in\mathbb{N}}$. It is immediate to show that

$$u^P = \sum_{q=0}^{P} u_q\phi_q \text{ with } u_q = \int u\phi_q\,\mathrm{d}\mathcal{P}_X, \tag{6}$$

is such that

$$\int_\Theta \left(u-u^P\right)^2\,\mathrm{d}\mathcal{P}_X \le \int_\Theta \left(u-v^P\right)^2\,\mathrm{d}\mathcal{P}_X,\ \forall v^P\in(\phi_k)_{k\in\{0,\dots,P\}}.$$

In other words, expansion (6) is the best one among all possible trials in $(\phi_k)_{k\in\{0,\dots,P\}}$ with respect to the L^2_Θ norm. In order to compute the coefficients $(u_q)_{q\in\{0,\dots,P\}}$, one can use the fact that u is the solution of an integro-differential equation with operators applying to t, $\mathbf{x}$ and $\mathbf{v}$. The gPC methodology consists in developing the unknown u of (4) on the polynomial basis

$$u^P(\mathbf{x},t,\mathbf{v},X) = \sum_{q=0}^{P} u_q(\mathbf{x},t,\mathbf{v})\phi_q(X), \tag{7}$$

and look for compatibility conditions on the coefficients $(u_k)_{k\in\{0,\dots,P\}}$ for u^P to be a good approximation of u. This is usually done by plugging (7) into (4) and by taking the moments of (4) against each orthonormal components $(\phi_q)_{q\in\{0,\dots,P\}}$. The reader interested in efficient resolutions for different physical applications is refered to [39, 40, 45, 34, 50, 13, 22, 29, 23, 42, 24, 27, 5, 7, 18, 58, 49, 21, 28, 52, 30, 31, 32, 16]. One finally obtains the moment model

$$\begin{cases} \forall q \text{ such that } 0\le q\le P, \\ \partial_t u_q(\mathbf{x},t,\mathbf{v}) + \mathbf{v}\cdot\nabla_{\mathbf{x}} u_q(\mathbf{x},t,\mathbf{v}) = -v\displaystyle\int\left(\sigma_t(\mathbf{x},t,\mathbf{v},X)\sum_{k\le p}u_k(\mathbf{x},t,\mathbf{v})\phi_k(X)\right)\phi_q(X)\,\mathrm{d}\mathcal{P}_X \\ \qquad\qquad + \displaystyle\iint v\left(\left(\sigma_s(\mathbf{x},t,\mathbf{v},\mathbf{v}',X)\sum_{k\le p}u_k(\mathbf{x},t,\mathbf{v})\phi_k(X)\right)\phi_q(X)\,\mathrm{d}\mathcal{P}_X\right)\mathrm{d}\mathbf{v}', \\ u_q(\mathbf{x},0,\mathbf{v}) = u_{0,q}(\mathbf{x},\mathbf{v}). \end{cases} \tag{8}$$

Since u is scalar, system (8) is a system of $(P+1)$ equations. It is a closed system in the sense that it has exactly $(P+1)$ equations and $(P+1)$ unknowns. In the following, system (8) will also be refered as the $P-$truncated gPC reduced model of (1) with standard closure (7).

It is reasonable to expect that (8) is an accurate approximation of the uncertain initial problem for large $P\gg 1$ (cf. Cameron-Martin's Theorem [10] or some generalization [17]). In fact, for this system, fast convergence rate have been practically observed in [47]. This paper is complementary to [47] in the sense that we here demonstrate the fast convergence of the $P-$truncated reduced models instead of only observing it *via* numerical experiments. We will indeed prove spectral accuracy under very general hypothesis in the next section 3.

3 Proof of spectral accuracy of the gPC reduced model

In this section we prove a result of spectral accuracy for the P-truncated gPC reduced models of the uncertain linear Boltzmann equation (8). We use a comparison method between a general approximated solution and a smooth exact solution to establish this result. The idea is similar to what has been proved in [14] for the scalar uncertain Burgers' equation for early times except it is applied to the uncertain linear Boltzmann equation which admits smoother solutions [25, 26, 3].

Let us assume the exact solution is smooth with respect to all variables

$$u \in L^\infty\left(\mathcal{D}\times[0,T]\times\mathcal{V}\times\Theta\right)\cap L^\infty\left(\mathcal{D}_{\text{per}}\times[0,T]\times\mathcal{V}_b : H^k(\Theta)\right). \tag{9}$$

In the above definition, $\mathcal{D}_{per}$ denotes a periodic spatial domain. Periodic boundary conditions are considered only for convenience, without loss of generality. Furthermore, $\mathcal{V}$ is the space of velocities and $\mathcal{V}_b$ recalls it is bounded (dealing with physical applications, the particles can not go beyond the speed of light for example). Finally, for all $k\in\mathbb{N}$ we have

$$H^k(\Theta)=\left\{u\in L^2_\Theta |\int\sum_{l=0}^{k}(u^{(l)})^2\,\mathrm{d}\mathcal{P}_X<\infty\right\},$$

where $u^{(l)}$ denotes the l^{th} derivative of u with respect to the uncertain variable. In other words, for solution $u(\mathbf{x},t,\mathbf{v},X)$, we have $u^{(l)}(\mathbf{x},t,\mathbf{v},\xi)=\partial^l_\xi u(\mathbf{x},t,\mathbf{v},\xi)$. The gPC reduced model of (1) of size $P+1$ is (we drop the dependencies for convenience)

$$\begin{cases}\partial_t u_0+\mathbf{v}\cdot\nabla_{\mathbf{x}}u_0 &= -v\displaystyle\int\left(\sigma_t\sum_{k\le p}u_k\phi_k\right)\phi_0\,\mathrm{d}\mathcal{P}_X+v\iint\left(\left(\sigma_s\sum_{k\le p}u_k\phi_k\right)\phi_0\,\mathrm{d}\mathcal{P}_X\right)\mathrm{d}\mathbf{v}',\\ \dots &\dots\\ \partial_t u_P+\mathbf{v}\cdot\nabla_{\mathbf{x}}u_P &= -v\displaystyle\int\left(\sigma_t\sum_{k\le p}u_k\phi_k\right)\phi_P\,\mathrm{d}\mathcal{P}_X+v\iint\left(\left(\sigma_s\sum_{k\le p}u_k\phi_k\right)\phi_P\,\mathrm{d}\mathcal{P}_X\right)\mathrm{d}\mathbf{v}'.\end{cases} \tag{10}$$

It is then possible to perform the scalar product $(u_0,...,u_P)^t\partial_t(u_0,...,u_P)$ to obtain an additional equation. Let us consider a smooth solution of (10), we get

$$\begin{aligned}&\partial_t\tfrac{\sum_{r=0}^P u_r^2}{2}+\mathbf{v}\cdot\nabla_{\mathbf{x}}\tfrac{\sum_{r=0}^P u_r^2}{2}=\\ &-v\int\sum_{q=0}^{P}\left(\sigma_t\sum_{k=0}^{P}u_k\phi_k\right)u_q\phi_q\,\mathrm{d}\mathcal{P}_X+v\iint\sum_{q=0}^{P}\left(\left(\sigma_s\sum_{k=0}^{P}u_k\phi_k\right)u_q\phi_q\,\mathrm{d}\mathcal{P}_X\right)\mathrm{d}\mathbf{v}'.\end{aligned} \tag{11}$$

After rearrangement of the collisional counterpart, it yields

$$\partial_t\sum_{r=0}^{P}\frac{u_r^2}{2}+\mathbf{v}\cdot\nabla_{\mathbf{x}}\sum_{r=0}^{P}\frac{u_r^2}{2}=-v\sum_{0\le k,q\le P}\int\sigma_t u_k\phi_k u_q\phi_q\,\mathrm{d}\mathcal{P}_X+\sum_{0\le k,q\le P}v\iint\sigma_s u_k\phi_k u_q\phi_q\,\mathrm{d}\mathcal{P}_X\,\mathrm{d}\mathbf{v}'. \tag{12}$$

Let us introduce

$$\sigma_s(\mathbf{x},t,\mathbf{v},X)=\int\sigma_s(\mathbf{x},t,\mathbf{v},\mathbf{v}',X)\,\mathrm{d}\mathbf{v}'\text{ and define }P_s(\mathbf{x},t,\mathbf{v},\mathbf{v}',X)=\frac{\sigma_s(\mathbf{x},t,\mathbf{v},\mathbf{v}',X)}{\sigma_s(\mathbf{x},t,\mathbf{v},X)}.$$

We have

$$\begin{aligned}&P_s(\mathbf{x},t,\mathbf{v},\mathbf{v}',X)>0, &&\forall(\mathbf{x},t,\mathbf{v},\mathbf{v}',X)\in\mathcal{D}\times[0,T]\times\mathcal{V}^2\times\Theta,\\ &\int P_s(\mathbf{x},t,\mathbf{v},\mathbf{v}',X)\,\mathrm{d}\mathbf{v}'=1, &&\forall(\mathbf{x},t,\mathbf{v},X)\in\mathcal{D}\times[0,T]\times\mathcal{V}\times\Theta.\end{aligned} \tag{13}$$

The difference $\sigma_a(\mathbf{x},t,\mathbf{v},X)=\sigma_t(\mathbf{x},t,\mathbf{v},X)-\sigma_s(\mathbf{x},t,\mathbf{v},X)$ corresponds to an absorption rate if positive, or a multiplication rate, if negative. We now suggested making few assumptions on the background media in which the particles are evolving.

Hypothesis 1 $\forall t\in[0,T]$, $\forall \mathbf{x}\in\mathcal{D}_{per}$, $\forall \mathbf{v}\in\mathcal{V}_b\subset\mathbb{R}^3$, $\forall X\in\Theta$

$$|v\sigma_t(\mathbf{x},t,\mathbf{v},X)|<\Sigma_t,\quad |v\sigma_s(\mathbf{x},t,\mathbf{v},X)|<\Sigma_s.$$

In other words, we have

$$||v\sigma_t||_{L^\infty(\mathcal{I}\times\Theta)}=\Sigma_t<\infty,\quad ||v\sigma_t||_{L^\infty(\mathcal{I}\times\Theta)}=\Sigma_s<\infty. \tag{14}$$

The above hypothesis expresses the fact we consider a background media leading to a finite number of collisions (term $v\sigma_t$) for every interval of times $[0,T]$ together with a finite multiplication rate (term relative to $v\sigma_s$) in $[0,T]$. Now, let us integrate (12) with respect to $\mathbf{x},t,\mathbf{v}$ on $\mathcal{D}_{per}\times[0,T]\times\mathcal{V}_b$, and use the above majorations. Let us define for convenience (we here introduce equivalent notations which will be useful later on)

$$\begin{aligned}
||u^P(t)||^2_{L^2(\mathcal{D}_{per}\times\mathcal{V}_b\times\Theta)} &= ||u^P(t)||^2_{L^2(\mathcal{I}\times\Theta)},\\
&= \iint\sum_{r=0}^{P} u_r^2(\mathbf{x},t,\mathbf{v})\,\mathrm{d}\mathbf{x}\,\mathrm{d}\mathbf{v},\\
&= \iiint\sum_{r=0}^{P} \left(u_r(\mathbf{x},t,\mathbf{v})\phi_r(\xi)\right)^2\,\mathrm{d}\mathbf{x}\,\mathrm{d}\mathbf{v}\,\mathrm{d}\mathcal{P}_X(\xi),\\
&= \iiint \left(u^P(\mathbf{x},t,\mathbf{v},X)\right)^2\,\mathrm{d}\mathbf{x}\,\mathrm{d}\mathbf{v}\,\mathrm{d}\mathcal{P}_X.
\end{aligned}$$

Integrating (12) with respect to $\mathbf{x}\in\mathcal{D}_{per}$ and $\mathbf{v}\in\mathcal{V}_b$ leads to

$$\begin{aligned}
&\frac{\mathrm{d}}{\mathrm{d}t}||u^P(t)||^2_{L^2(\mathcal{I}\times\Theta)}\\
&\le 2\Sigma_t\iiint\sum_{k=0}^{P}u_k^2+2\Sigma_s\sum_{0\le k,q\le P}\iint\iint\left(u_k(\mathbf{x},t,\mathbf{v}')\phi_k u_q(\mathbf{x},t,\mathbf{v})\phi_q\right)\,\mathrm{d}\mathcal{P}_X\,\mathrm{d}\mathbf{v}'\,\mathrm{d}\mathbf{v}\,\mathrm{d}\mathbf{x},\\
&\le 2\Sigma_t||u^P(t)||^2_{L^2(\mathcal{I}\times\Theta)}\\
&\qquad +2\Sigma_s\sum_{0\le k,q\le P}\int\left[\int\left(\int u_k(\mathbf{x},t,\mathbf{v}')\,\mathrm{d}\mathbf{v}'\int u_q(\mathbf{x},t,\mathbf{v})\,\mathrm{d}\mathbf{v}\right)\,\mathrm{d}\mathbf{x}\right]\phi_k\phi_q\,\mathrm{d}\mathcal{P}_X,\\
&\le 2\Sigma_t||u^P(t)||^2_{L^2(\mathcal{I}\times\Theta)}+2\Sigma_s\sum_{k=0}^{P}\int\left(\int u_k(\mathbf{x},t,\mathbf{v})\,\mathrm{d}\mathbf{v}\right)^2\,\mathrm{d}\mathbf{x}.
\end{aligned}\tag{15}$$

Finally, Jensen's inequality ensures we have

$$\partial_t||u^P(t)||^2_{L^2(\mathcal{I}\times\Theta)}\le 2(\Sigma_t+\Sigma_s)||u^P(t)||^2_{L^2(\mathcal{I}\times\Theta)} \tag{16}$$

Gronwall's theorem allows obtaining the *a priori* bound

$$\left\|u^P(t)\right\|_{L^2(\mathcal{I}\times\Theta)}\le e^{2(\Sigma_t+\Sigma_s)t}\left\|u_0^P\right\|_{L^2(\mathcal{I}\times\Theta)}. \tag{17}$$

It is therefore natural to seek solutions of the uncertain linear Boltzmann equation in the space $L^\infty([0,T]:L^2(\mathcal{I}\times\Theta))$. Here is the main result of this paper.

Theorem 1 (Convergence of the $P-$truncated gPC reduced model approximation) *Spectral accuracy holds in the following sense: for all $k\in\mathbb{N}$ such that $u\in H^k(\Theta)$, there exists a constant D_k such that $\forall t\in[0,T]$*

$$\left\|u(t)-u^P(t)\right\|^2_{L^2(\mathcal{I}\times\Theta)}\le e^{2(\Sigma_t+\Sigma_s)t}\left(\left\|u_0-u_0^P\right\|^2_{L^2(\mathcal{I}\times\Theta)}+2(\Sigma_s+\Sigma_t)t||u_0^2||_{L^2(\mathcal{I}\times\Theta)}\frac{D_k}{P^k}\right). \tag{18}$$

Before prooving the above result, we would like to comment on it. Obviously, with hypothesis 1, we have $\Sigma_s + \Sigma_t \geq 0$. As a consequence, the term $e^{2(\Sigma_t+\Sigma_s)t}$ may be a fast increasing factor. So, first, the term depending on the error on the initial condition, i.e. $e^{2(\Sigma_t+\Sigma_s)t}\left\|u_0 - u_0^P\right\|^2_{L^2(\mathcal{I}\times\Theta)}$, shows that any small error on the initial condition can be exponentially amplified. On other words, care must be taken to make sure the P-truncated approximation of the initial condition is accurate. The gPC framework [54, 56, 60, 59, 17], in opposition to the PC one [57, 10, 24], has been introduced precisely to this purpose: the initial polynomial basis must at least be able to fit accurately to the initial uncertain condition to ensure a converging behaviour and avoid stagnation[3]. Second, the remaining term, i.e. $2(\Sigma_s + \Sigma_t)te^{2(\Sigma_t+\Sigma_s)t}||u_0^2||_{L^2(\mathcal{I}\times\Theta)}\frac{D_k}{P^k}$, shows that even if care has been taken to make sure $\left\|u_0 - u_0^P\right\|^2_{L^2(\mathcal{I}\times\Theta)} = 0$, the error can still grow quickly with time. It can be *theoretically* compensated with an increasing polynomial order P. The smoother the solution, the more efficient the increase of P. The fact the gPC reduced models presents some difficulties with *long term integration* is also well-known in the literature [55, 53, 20]: it is here theoretically recovered. Of course, in practice, increasing P is not straightforward as the reduced models will be harder and harder to solve as P grows, especially in high stochastic dimensions (this is commonly called the curse of dimensionality) [4, 5, 12]. Still, in practice, with the following numerical example, we will show that the above bounds, even if enough to prove the fast convergence of the gPC reduced models for the uncertain linear Boltzmann equation, may be pessimistic and non-optimal. But before tackling numerical example, let us proove theorem 1.

Proof Assume u is a continuous solution of (4) and $u^P = \sum_{k=0}^P u_k\phi_k$ of the form (6) whose coefficients $(u_q)_{q\in\{0,\dots,P\}}$ solve (8). Then we suggest building an estimate of (we drop the dependencies for conciseness)

$$\partial_t \int_\Theta \frac{(u^P-u)^2}{2}\,\mathrm{d}\mathcal{P}_X = \int_\Theta \left(\partial_t\frac{(u^P)^2}{2} - u^P\partial_t u - u\partial_t u^P + \partial_t\frac{u^2}{2}\right)\mathrm{d}\mathcal{P}_X.$$

Unknowns u and $(u_0,\dots,u_P)^t$ being strong solutions of (4) and (8), we have

$$\begin{aligned}\partial_t \int_\Theta \frac{(u^P-u)^2}{2} = \quad & -\int_\Theta \mathbf{v}\cdot\nabla_{\mathbf{x}}\frac{u^2}{2} - \int_\Theta v\sigma_t u^2 + v\int_\Theta \sigma_s u\int u \\ & + \int_\Theta u^P\mathbf{v}\cdot\nabla_{\mathbf{x}}u + v\int_\Theta \sigma_t u^P u - v\int_\Theta \sigma_s u^P\int u \\ & + \int_\Theta u\mathbf{v}\cdot\nabla_{\mathbf{x}}u^P + v\int_\Theta \sigma_t u^P u - v\int_\Theta \sigma_s u\int u^P \\ & - \int_\Theta \mathbf{v}\cdot\nabla_{\mathbf{x}}\frac{(u^P)^2}{2} - v\int_\Theta \sigma_t (u^P)^2 + v\int_\Theta \sigma_s u^P\int u^P.\end{aligned}$$

Integration with respect to $\mathbf{x}\in\mathcal{D}_{per}, \mathbf{v}\in\mathcal{V}_b$ yields

$$\begin{aligned}\frac{\mathrm{d}}{\mathrm{d}t}\iiint_\Theta \frac{(u^P-u)^2}{2} = \quad & -\cancel{\iiint_\Theta \mathbf{v}\cdot\nabla_{\mathbf{x}}\frac{u^2}{2}} - \iiint_\Theta v\sigma_t u^2 + v\iiint_\Theta \sigma_s u\int u \\ & + \iiint_\Theta u^P\mathbf{v}\cdot\nabla_{\mathbf{x}}u + \iiint_\Theta v\sigma_t u^P u - v\iiint_\Theta \sigma_s u^P\int u \\ & + \iiint_\Theta u\mathbf{v}\cdot\nabla_{\mathbf{x}}u^P + \iiint_\Theta v\sigma_t u^P u - v\iiint_\Theta \sigma_s u\int u^P \\ & - \cancel{\iiint_\Theta \mathbf{v}\cdot\nabla_{\mathbf{x}}\frac{(u^P)^2}{2}} - \iiint_\Theta v\sigma_t (u^P)^2 + v\iiint_\Theta \sigma_s u^P\int u^P.\end{aligned}$$

The terms in the above expression cancel due to the hypothesis of having periodic boundary conditions. For the same reason we have $\int_{\mathcal{D}_{per}} u^P\nabla_{\mathbf{x}}u\,\mathrm{d}\mathbf{x} = \cancel{\int_{\partial\mathcal{D}_{per}} (u^P u)\cdot n\,\mathrm{d}\sigma} - \int_{\mathcal{D}_{per}} u\nabla_{\mathbf{x}}u^P\,\mathrm{d}\mathbf{x}$ so that the

[3] Indeed, if $\left\|u_0 - u_0^P\right\|^2_{L^2(\mathcal{I}\times\Theta)} = C_0 \neq 0$, then $\left\|u(t) - u^P(t)\right\|^2_{L^2(\mathcal{I}\times\Theta)} \underset{P\to\infty}{\longrightarrow} C_0 e^{2(\Sigma_s+\Sigma_t)t}$ for fixed time t.

previous expression becomes

$$\begin{aligned}\frac{\mathrm{d}}{\mathrm{d}t}\iiint_\Theta \frac{(u^P-u)^2}{2} = & -\iiint_\Theta v\sigma_t u^2 + \iiint_\Theta v\sigma_s u\int u \\ & +\iiint_\Theta v\sigma_t u^P u - \iiint_\Theta v\sigma_s u^P\int u \\ & +\iiint_\Theta v\sigma_t u^P u - \iiint_\Theta v\sigma_s u\int u^P \\ & -\iiint_\Theta v\sigma_t (u^P)^2 + \iiint_\Theta v\sigma_s u^P\int u^P.\end{aligned}$$

Let us now define $\pi_P u$ the orthogonal projector of u solution to (4) in $L^2(\Theta)$ onto the space $(\phi_k)_{k\in\{0,\dots,P\}}$. The previous expression can be equivalently rewritten

$$\begin{aligned}\frac{\mathrm{d}}{\mathrm{d}t}\iiint_\Theta \frac{(u^P-u)^2}{2} = & -\iiint_\Theta v\sigma_t u^2 & +\iiint_\Theta v\sigma_s u\int u \\ & +\iiint_\Theta v\sigma_t u^P\pi_P u & -\iiint_\Theta v\sigma_s u^P\int \pi_P u \\ & +\iiint_\Theta v\sigma_t u^P\pi_P u & -\iiint_\Theta v\sigma_s \pi_P u\int u^P \\ & -\iiint_\Theta v\sigma_t (u^P)^2 & +\iiint_\Theta v\sigma_s u^P\int u^P.\end{aligned}$$

Let us now rearrange the terms as

$$\begin{aligned}&\frac{\mathrm{d}}{\mathrm{d}t}\iiint_\Theta \frac{(u^P-u)^2}{2} = \\ &\quad +\iiint_\Theta v\sigma_t\left(2u^P(\pi_P u-u)-(u^P-u)^2\right) \quad +\iiint_\Theta v\sigma_s\left((u-u^P)\left[\int u-\int u^P\right]\right) \\ &\qquad\qquad +\iiint_\Theta v\sigma_s\left(-u^P\int(\pi_P u-u)-(\pi_P u-u)\int u^P\right).\end{aligned}$$

From hypothesis (1), we obtain

$$\begin{aligned}\frac{\mathrm{d}}{\mathrm{d}t}\iiint_\Theta \frac{(u^P-u)^2}{2} \le & +2\Sigma_t\left|\iiint_\Theta u^P(\pi_P u-u)\right| & +\Sigma_s\iint_\Theta\left(\int(u-u^P)\right)^2 \\ & +\Sigma_t\iiint_\Theta (u^P-u)^2 & +2\Sigma_s\left|\iint_\Theta\left(\int u^P\int(\pi_P u-u)\right)\right|.\end{aligned}$$

From Jensen's inequality, we have

$$\begin{aligned}\frac{\mathrm{d}}{\mathrm{d}t}\iiint_\Theta \frac{(u^P-u)^2}{2} \le & +2(\Sigma_t+\Sigma_s)\iiint_\Theta \frac{(u-u^P)^2}{2} & +2\Sigma_t\left|\iiint_\Theta u^P(\pi_P u-u)\right| \\ & & +2\Sigma_s\left|\iint_\Theta\left(\int u^P\int(\pi_P u-u)\right)\right|,\end{aligned}$$

to finally get (Hölder inequality)

$$\begin{aligned}\frac{d}{dt}\left\|(u-u^P)(t)\right\|^2_{L^2(\mathcal{I}\times\Theta)} \le & +2(\Sigma_t+\Sigma_s)||(u-u^P)(t)||^2_{L^2(\mathcal{I}\times\Theta)} \\ & +2(\Sigma_t+\Sigma_s)||u^P(t)||_{L^2(\mathcal{I}\times\Theta)}\times||(\pi_P u-u)(t)||_{L^\infty(\mathcal{I}\times\Theta)}.\end{aligned}$$

Let us now work on the last term of the previous expression. Thanks to (17), we are able to bound

$$\begin{aligned}\frac{d}{dt}\left\|(u-u^P)(t)\right\|^2_{L^2(\mathcal{I}\times\Theta)} \le & +2(\Sigma_t+\Sigma_s)||(u-u^P)(t)||^2_{L^2(\mathcal{I}\times\Theta)} \\ & +2(\Sigma_t+\Sigma_s)e^{2(\Sigma_s+\Sigma_t)t}||u_0^P||_{L^2(\mathcal{I}\times\Theta)}\times||\pi_P u-u||_{L^\infty(\mathcal{I}\times\Theta)}.\end{aligned} \tag{19}$$

This means it only remains to be able to deal with the L^∞-norm the $\pi_P u - u$ to conclude.

In the following for simplicity of notations, we assume that $X \in \mathbb{R}^{Q=1}$, but the reasoning can be carried on in any dimension at the price of more tedious calculations. Now, the truncation of the expansion gives

$$u(\mathbf{x},t,\mathbf{v},X) - \pi_P u(\mathbf{x},t,\mathbf{v},X) = \sum_{n=P+1}^{\infty} \phi_n(X) \int u(\mathbf{x},t,\mathbf{v},X)\phi_n(X)\,\mathrm{d}\mathcal{P}_X,$$

Furthermore, orthonormal polynomials $(\phi_k)_{k\in\{0,\dots,P\}}$ are known to be the eigenvectors of the eigenproblem (see [2])

$$\left(Q(\xi)\frac{\mathrm{d}^2}{\mathrm{d}\xi^2} + L(\xi)\frac{\mathrm{d}}{\mathrm{d}\xi}\right)\phi(\xi) = \lambda\phi(\xi), \tag{20}$$

where Q and L are respectively second and first order polynomials and $\lambda_k = -k(\frac{k-1}{2}Q'' + L'), \forall k \in \mathbb{N}$. For example, for Legendre polynomials, $Q(\xi) = 1-\xi^2$, $L(\xi) = -2\xi$ and the eigenvalues are $k(k+1), \forall k \in \mathbb{N}$. For Hermite polynomials (related to the gaussian distribution), $Q(\xi) = 1$, $L(\xi) = -2\xi$ and $\lambda_k = 2k, \forall k \in \mathbb{N}$. As a consequence, we have

$$\left(Q(\xi)\frac{\mathrm{d}^2}{\mathrm{d}\xi^2} + L(\xi)\frac{\mathrm{d}}{\mathrm{d}\xi}\right)[u(\mathbf{x},t,\mathbf{v},\xi) - \pi_P u(\mathbf{x},t,\mathbf{v},\xi)] = \sum_{k=P+1}^{\infty} \lambda_k\phi_k(\xi) \int u(\mathbf{x},t,\mathbf{v},X)\phi_k(X)\,\mathrm{d}\mathcal{P}_X.$$

Since the derivative of u with respect to ξ are bounded in L^2_Θ up to order k by hypothesis (9), we have

$$\sum_{j=P+1}^{\infty}\left[\int u(\mathbf{x},t,\mathbf{v},X)\phi_k(X)\,\mathrm{d}\mathcal{P}_X\right]^2 \lambda_j^{2m} < \infty, \qquad \forall m \in \{0,\dots,\lfloor\frac{k}{2}\rfloor\}, \quad \forall t\in[0,T],\ (\mathbf{x},\mathbf{v})\in\mathcal{I}. \tag{21}$$

Finally, one has the bound for all $t \in [0,T]$, $(\mathbf{x},\mathbf{v}) \in \mathcal{I}$ and $\forall m \in \{0,\dots,\lfloor\frac{k}{2}\rfloor\}$

$$\begin{aligned}
&\|u(\mathbf{x},t,\mathbf{v},\cdot) - \pi_P u(\mathbf{x},t,\mathbf{v},\cdot)\|_{L^\infty(\Theta)} \\
&\qquad \le \sum_{n=P+1}^{\infty}\left|\int u(\mathbf{x},t,\mathbf{v},X)\phi_k(X)\,\mathrm{d}\mathcal{P}_X\right| \|\phi_n\|_{L^\infty(\Theta)} \\
&\qquad \le \left(\sum_{n=P+1}^{\infty}\left[\int u(\mathbf{x},t,\mathbf{v},X)\phi_k(X)\,\mathrm{d}\mathcal{P}_X\right]^2 \lambda_n^{2m}\right)^{\frac{1}{2}} \left(\sum_{n=P+1}^{\infty}\frac{\|\phi_n\|^2_{L^\infty(\Theta)}}{\lambda_n^{2m}}\right)^{\frac{1}{2}}.
\end{aligned} \tag{22}$$

The first sum is bounded, cf. (21). The second term deserves some more attention. Without loss of generality (see (3) and the relative discussion), we can always consider that, up to change of variable (3), X is uniformly distributed and $(\phi_k^L)_{k\in\mathbb{N}}$ are the Legendre polynomials. Under the previous condition, we have the bound [2] $\forall n \in \mathbb{N}$

$$\|\phi_n^L\|_{L^\infty(\Theta)} \le C(n+1)^{\frac{1}{2}}. \tag{23}$$

Remark 3.1 *Note that in the above lines, care has been taken to have resort to the change of variable (3) and Legendre polynomials the later possible. In practice, avoiding this change of variable is complex, especially if X is an unbounded random variable. To be able to conclude for an arbitrary random variable X*[4]*, we would both need to show that $\|\phi_n^X\|_{L^\infty(\Theta)}$ is bounded and, more than bounded, grows with n less quickly than λ_n^k. In [37], the authors study conditions on $\mathrm{d}\mathcal{P}_X$ to obtain bounds of $\|\phi_n^X(\xi)\frac{\mathrm{d}\mathcal{P}_X}{\mathrm{d}\xi}(\xi)\|_{L^\infty(\Theta)}$ defined on an unbounded space. Note that those bounds does not grow too fast*

[4]together with its associated polynomial basis $(\phi_k^X)_{k\in\mathbb{N}}$, orthonormal with respect to the scalar product defined by $\mathrm{d}\mathcal{P}_X$.

with n, see [37]. In other words, the equivalent of (23) for arbitrary weighted polynomials $(\phi_k^X \frac{\mathrm{d}\mathcal{P}_X}{\mathrm{d}\xi})_{k\in\mathbb{N}}$ may be at hand. But the crucial step remains to be able to go from (22) to and inequality involving $\|\phi_n^X(\xi)\frac{\mathrm{d}\mathcal{P}_X}{\mathrm{d}\xi}(\xi)\|_{L^\infty(\Theta)}$. To our knowledge, this point is not straightforwar but would stand for the last step to conclude of the spectral convergence of the gPC based reduced models without having resort to uniform random variable/Legendre polynomials. Avoiding having resort to change of variable (3) may lead to finer bounds for an arbitrary random vector X.

As a consequence, with the above (uniform/Legendre) hypothesis and (23), there exists a constant C_k such that

$$\|u(\mathbf{x},t,\mathbf{v},\cdot)-\pi_P u(\mathbf{x},t,\mathbf{v},\cdot)\|_{L^\infty(\Theta)} \leq \frac{C_k}{P^k} \tag{24}$$

Finally, putting together (19)–(24) and invoking Gronwall's theorem allows ending the proof of theorem 1. ■

In the following section, we present few numerical results. Most of them confirms the result of theorem 1. Some of them aim at going beyond it and tackle perspectives and open problems.

4 Numerical application

In this last section, we present few numerical results obtained from the resolution of $P-$truncated gPC reduced models. In section 4.1, we consider a homogeneous configuration for which an analytical solution is available. In section 4.2, we consider a test-case for which, to our knowledge, no analytical solutions are available. The results are obtained thanks to the numerical scheme presented in [47]. Note that we here aim at emphasizing the fast convergence of the gPC based reduced models as proved in theorem 1. For this, it enough considering monodimensional uncertain problems (i.e. $Q=1$) and simple statistical observables such as the mean and the variance. The reader interested a high dimensional resolution of (4) together with more exotic statistical observables (Sobol indices for example, for sensitivity analysis) can refer to [47].

4.1 A first simple homogeneous uncertain configuration

In this first numerical section, we compare the results obtained from $P-$truncated gPC reduced models to an analytical solution. We aim at numerically recovering the fast convergence rate demonstrated in theorem 1. The test-problem has already been introduced in [47] but we tackle it from a different

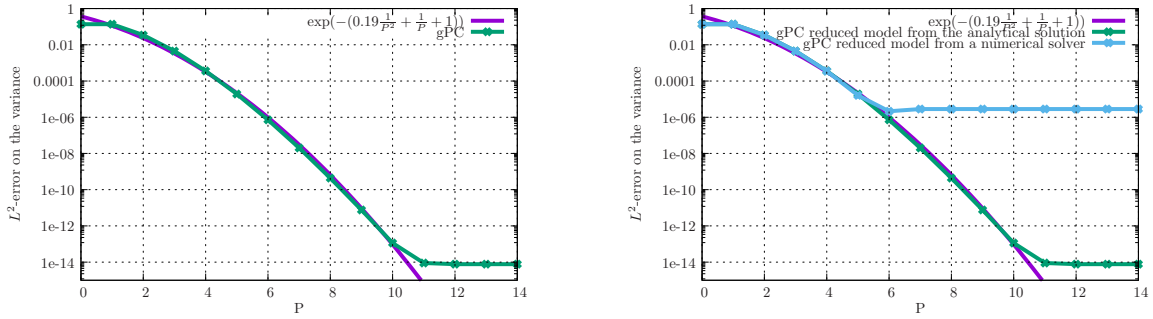

Figure 1: Left: convergence study with respect to P obtained with an analytical solutiion of the gPC reduced model. The plot also display the function $P \longrightarrow \exp(-(0.19\frac{1}{P^2}+\frac{1}{P}+1))$. Right: convergence study with respect to P obtained with numerically computed solution of the gPC reduced model.

point of view (convergence with respect to P here).

Let us consider a monokinetic (i.e. $v = 1$) homogeneous (i.e. $u(\mathbf{x}, t, \mathbf{v}, X) = u(t, \omega, X)$) configuration. We assume the uncertainty, one-dimensional here for the sake of simplicity, affects the scattering cross-sections $\sigma_s = \overline{\sigma}_s + \hat{\sigma}_s X$, where $X \sim \mathcal{U}[-1, 1]$. Of course, $\hat{\sigma}_s$ is closely related to the variance of the uncertain scattering cross-section. Let us introduce $U(t, X) = \int u(t, \omega, X)\, \mathrm{d}\omega$. In the previously described configuration, the uncertain linear Boltzmann equation resumes to the following stochastic ordinary differential equation (ODE)

$$\begin{cases} \partial_t U(t, X) + v\sigma_t U(t, X) = v\sigma_s(X) U(t, X), \\ U(0) = U_0. \end{cases} \tag{25}$$

Introduce $\sigma_a = \sigma_t - \sigma_s$, then the solution is given by

$$U(t, X) = U_0 e^{-v\sigma_a(X)t} = U_0 e^{-v(\sigma_t - \overline{\sigma}_s - \hat{\sigma}_s X)t} = U_0 e^{-v(\overline{\sigma}_a - \hat{\sigma}_s X)t}. \tag{26}$$

The quantity $U(t, X)$ is a random variable indexed by time t, i.e. it is a stochastic process. In this case, mean and variance of the stochastic process (26) can be computed analytically and are given by

$$\begin{aligned} M_1^U(t) = \mathbb{E}[U(t, X)] &= \tfrac{1}{2} U_0 e^{-v\overline{\sigma}_a t} \frac{e^{v\hat{\sigma}_s t} - e^{-v\hat{\sigma}_s t}}{\hat{\sigma}_s t v}, \\ M_2^U(t) = \mathbb{E}[U^2(t, X)] &= \tfrac{1}{4} U_0^2 e^{-2v\overline{\sigma}_a t} \frac{e^{2v\hat{\sigma}_s t} - e^{-2v\hat{\sigma}_s t}}{\hat{\sigma}_s t v}, \\ \mathbb{V}[U](t) &= M_2^U(t) - (M_1^U(t))^2. \end{aligned} \tag{27}$$

Of course, higher order moments, probability of failure, complete characterisation of the probability density function of the stochastic process can be calculated but in figure 1 we focus on the variance $\mathbb{V}[U](t)$ to perform the convergence studies.
Our aim now is to compare the results obtained from a $P-$truncated gPC based reduced model and the analytical ones. In this particular configuration, the reduced model (10) resumes to a system of coupled ODEs

$$\partial_t \begin{pmatrix} U_0(t) \\ \dots \\ U_P(t) \end{pmatrix} = \Sigma_a \begin{pmatrix} U_0(t) \\ \dots \\ U_P(t) \end{pmatrix}, \tag{28}$$

with

$$\Sigma_a = \begin{pmatrix} \sum_{k=0}^{P} \int \sigma_a \phi_0 \phi_0 \, \mathrm{d}\mathcal{P}_X & & \sum_{k=0}^{P} \int \sigma_a \phi_0 \phi_P \, \mathrm{d}\mathcal{P}_X \\ \dots & \sum_{k=0}^{P} \int \sigma_a \phi_i \phi_j \, \mathrm{d}\mathcal{P}_X & \dots \\ \sum_{k=0}^{P} \int \sigma_a \phi_P \phi_0 \, \mathrm{d}\mathcal{P}_X & & \sum_{k=0}^{P} \int \sigma_a \phi_P \phi_P \, \mathrm{d}\mathcal{P}_X \end{pmatrix}.$$

The solution of the above system is the exponential of matrix Σ_a with initial condition $(U_0^0, ..., U_P^0)^t$. It can be computed analytically with any algebraic computation software for arbitrary order P. Note that we also verified that the use of fine non intrusive resolution (with Gauss-Legendre points) gives equivalent results. The results presented in figure 1 compare the variance obtained from the analytical solution (27) and the variance obtained from the analytical solution of (28). Figure 1 displays three curves:

– the first one (on both figure 1 left and right) corresponds to a convergence study with respect to P of the L^2-norm of the error of U solution of (25) and $U^P = \sum_{k=0}^{P} U_k \phi_k$ where $(U_0, ..., U_P)^t$ is solution of (28).

– The second one (on both figure 1 left and right) corresponds to a plot of function $P \longrightarrow \exp(-(0.19\frac{1}{P^2} + \frac{1}{P} + 1))$.

– The last curve (only on figure 1 right) corresponds to the same convergence study except $(U_0, ..., U_P)^t$, solution of (28), is obtained numerically. We use an explicit Euler scheme of time step $\Delta t = 10^{-7}$.

Note that in practice, we take $v = 1, U_0 = 1, \sigma_t = 1, \overline{\sigma}_s = 0.8, \hat{\sigma}_s = 0.3$. The first curve, the convergence study comparing the analytical solutions of (25) and (28), testifies of a fast converging behaviour of U^P toward U as P increases. Machine accuracy is reached as soon as $P = 10$. The curve $P \longrightarrow \exp(-(0.19\frac{1}{P^2} + \frac{1}{P} + 1))$ perfectly fits the latter, up to order $P = 10$. It means the convergence rate observed here is even faster than the one predicted by theorem 1. Of course, theorem 1 has been proved in more general conditions. But the latter numerical result also probably shows the bounds of theorem 1 are not optimal, at least for homogeneous problems. The convergence study obtained from a numerically solved system (28) (figure 1 right) presents the same behaviour as the analytical convergence curve up to order $P = 6$: for higher truncation order, the solution is $\mathcal{O}(\Delta t) \approx 10^{-6}$ and P is not anymore the constraining parameter.

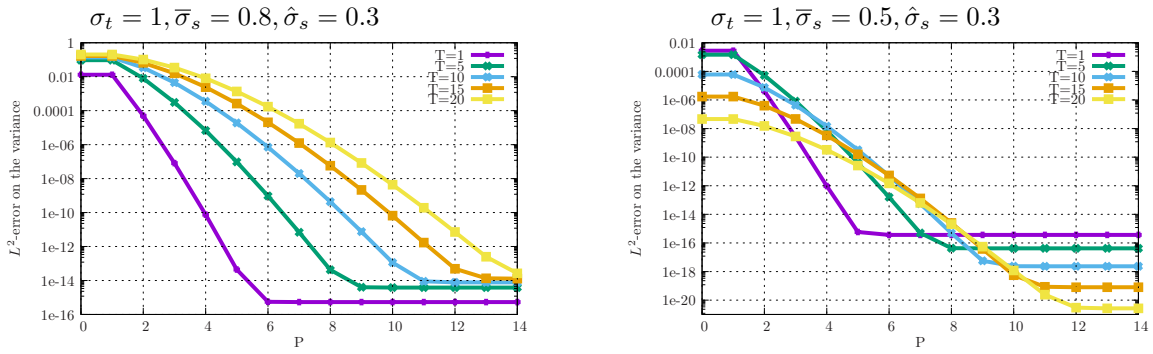

Figure 2: Left: convergence study with respect to P obtained with an analytical gPC reduced model and a numerically obtained one for parameters $\sigma_t = 1, \overline{\sigma}_s = 0.8, \hat{\sigma}_s = 0.3$ for several final times $T = 1, 5, 10, 20$. Right convergence study with respect to P obtained with an analytical gPC reduced model and a numerically obtained one for parameters $\sigma_t = 1, \overline{\sigma}_s = 0.5, \hat{\sigma}_s = 0.3$ for several final times $T = 1, 5, 10, 20$.

Figure 2 presents the same kind of convergence studies for different final times $T = 1, 5, 10, 20$ and for different values of $\overline{\sigma}_s$ controling the variability of the uncertainty in the scattering cross-section. ($\overline{\sigma}_s = 0.8$ for the left picture, $\overline{\sigma}_s = 0.5$ for the right one). Let us begin with figure 2 (left). It corresponds to the case $\sigma_t = 1, \overline{\sigma}_s = 0.8, \hat{\sigma}_s = 0.3$: for these values of cross-sections, there exists some realizations X such that $\overline{\sigma}_s + \hat{\sigma}_s X > \sigma_t$ with $\mathbb{P}(\overline{\sigma}_s + \hat{\sigma}_s X > \sigma_t) > 0$. In other words, the medium can be multiplicative with a non-negligible probability. Figure 2 (left) presents the convergence studies obtained with the previous parameters for different final times T. Once again, we recover the behaviour predicted by theorem 1: first, spectral convergence is ensured independently of the final time T. Second, the later the final time T, the higher the error on the variance: $\forall P \in \{0, ..., 14\}$, the error for early times is lower than the error for later times. Still, acceptable error remains reachable as, for example, $P = 10$ still ensures an accuracy below 10^{-8} (which is two decades below the numerical error $\mathcal{O}(\Delta t) = 10^{-6}$ for example). Figure 2 (right) presents the same convergence studies but with $\sigma_t = 1, \overline{\sigma}_s = 0.5, \hat{\sigma}_s = 0.3$: for these values of cross-sections, the set $\{X \in [-1, 1] | \overline{\sigma}_s + \hat{\sigma}_s X > \sigma_t\}$ is such that $\mathbb{P}(\overline{\sigma}_s + \hat{\sigma}_s X > \sigma_t) = 0$. In other words, the medium can never be multiplicative, it is absorbing with probability 1. The convergence studies of figure 2 (right) tend to put forward the fact the coefficient in the exponential in (18) is negative whereas this possibility is not predicted by theorem 1. As a consequence, the error, in this case, decreases with time: for example, an accuracy of 10^{-8}

is reached as soon as $P = 4$ for $T \leq 20$. In this simple uncertain configuration, the reduced models behave even better than predicted by (18) in theorem 1.

In the next section, we consider a test-case for which, to our knowledge, no analytical solution is available. We will have resort to the numerical scheme described in [47].

4.2 Taking into account uncertainties in the scattering cross-section

Let us now tackle a new test-problem for which an analytical solution is not available despite the relative simplicity of the configuration. Note that care has been taken to consider a configuration different from the ones of [47]. We aim at making this paper and [47] complementary.

Let us present the detail of the next study:

- let us consider $\mathbf{x} = x \in \mathcal{D} = [0, 1]$.
- We assume the particles are monokinetic with $v = 1$.
- Besides, we assume that the medium is only diffusive (no absorption, i.e. $\sigma_t = \sigma_s$) and the cross-sections are deterministic. We choose $\sigma_s = \sigma_t = 1$.
- We here want to take into account uncertainties in the distribution of the scattering angle P, see expression (13). Let us consider a monodimensional uncertain parameter (i.e. $Q = 1$) and assume it is uniformly distributed in $[-1, 1]$, i.e. $X \sim \mathcal{U}([-1, 1])$. The uncertain parameter X affects the outer angular distribution. With the above hypothesis (monodimensional and monokinetic) we have $P_s(x, t, \mathbf{v}, \mathbf{v}', X) = P_s(\omega', X)$. Furthermore in this test-problem, we assume P_s is not isotropic and uncertain. We assume we have

  $$P_s(\omega', X)\, \mathrm{d}\omega' = \mathbf{1}_{[0,U(X)]}(\omega'),$$

  where $X \longrightarrow U(X) = 0.8\frac{(X+1)}{2}$ maps X in $[-1, 1]$ into a uniformly distributed random variable $U(X)$ in $[0, 0.8]$. As a consequence, the scattering is always anisotropic and depending on the realizations of X, the scattering angle can be sampled in a narrower band than $[0, 0.8]$. Note that $\omega' \longrightarrow P_s(\omega', X)$ is positive and sums up to 1, $\forall X \in [-1, 1]$: it is always a probability density function and the scattering angle always has sense. The expression of the scattering angle distribution may appear singular for the reader familiar with the linear Boltzmann equation (neutronics or photonics for example). At this stage of the discussion, we can already explain it has been chosen simple (for ease of reproduction of the numerical results) and so that the convergence behaviour (this will be emphasized later on) is not too fast (see remark 4.1).
- The initial condition is a Heaviside between 0 and $\frac{1}{50}$, i.e. we have a deterministic initial condition given by $u_0(x, \omega) = \mathbf{1}_{[0,\frac{1}{50}]}(x)$.

In this particular case, (4) resumes to

$$\begin{cases} \partial_t u(x, t, \omega, X) + v\omega\partial_x u(x, t, \omega, X) = -v\sigma_s u(x, t, \omega, X) + v\sigma_s \displaystyle\int P_s(\omega', X) u(x, t, \omega', X)\, \mathrm{d}\omega', \\ u(x, 0, \omega) = u_0(x) = \mathbf{1}_{[0,\frac{1}{50}]}(x). \end{cases} \tag{29}$$

Note that in the next study, we take specular boundary condition on both sides of domain $\mathcal{D} = [0, 1]$. In other words, the particles hit walls with perfect reflection at $x = 0$ and $x = 1$. The computation has been made by the Monte-Carlo scheme described in [47]. It has $N_x = 50$ cells, but they are only used for visualisation. The most important numerical parameter for such a numerical solver is the number of MC particles $N_{MC} = 2.8 \times 10^7$ (see [47] for more details on the resolution scheme).

Figure 3 presents the numerical results obtained in this configuration. Let us introduce notation $U(x,t,X) = \int u(x,t,\omega,X)\,\mathrm{d}\omega$. Let us furthermore introduce $\forall k \in \{0,...,P\}$

$$U_k(x,t) = \int u_k(x,t,\omega)\,\mathrm{d}\omega = \iint u(x,t,\omega,X)\phi_k(X)\,\mathrm{d}\mathcal{P}_X\,\mathrm{d}\omega. \tag{30}$$

Then $U^P(x,t) = \sum_{k=0}^{P} U_k(x,t)\phi_k(X)$ is an approximation of $U(x,t)$ obtained from the numerical resolution of reduced model (8). Approximations of the mean and variance are easily obtained from U^P as we have

$$\begin{aligned} &\mathbb{E}[U](x,t) \approx \mathbb{E}[U^P](x,t) = U_0(x,t), \\ &\mathbb{V}[U](x,t) \approx \mathbb{V}[U^P](x,t) = \sum_{k=1}^{P} U_k^2(x,t). \end{aligned} \tag{31}$$

Many other classical statistical quantities can be obtained from post-treatments of the gPC coefficients, see [6]. Some examples (Sobol indices) are given in [47].

Figure 3 (left) displays $\mathbb{E}[U^{P=7}](x,t)$, $\mathbb{V}[U^{P=7}](x,t)$ and N realizations of $U^{P=7}(x,t,X)$ for $N = 100$ uniformly distributed $(X_i)_{i\in\{1,...,N\}} \sim \mathcal{U}([-1,1])$ for several times $t \in \{0.1, 0.5, 1.0, 2.0\}$. Note that on figure 3 (left), the left axis corresponds to the scale for the mean and the realizations whereas the right axis corresponds to the scale for the variance. Figure 3 (right) presents a convergence study with respect to P for the spatial profiles of the variance.

Let us first focus on figure 3 (left) and on a description of the test-case. The initial condition is deterministic and consists in a Heaviside of particles along the left wall. We begin by the description of the average behaviour, the mean $\mathbb{E}[U^{P=7}](x,t)$. At time $t = 0.1$ (figure 3 top left), particles are evolving in the random medium. The bulk is propagating toward the right hand side but some particles remain in the vicinity of the wall due to the scattering they encounter. As time passes, the average population of particles goes toward the right wall and are reflected toward the center of the domain. From a variance point of view, uncertainties are affecting the particles as soon as $t > 0$. The area of highest variance remains in the vicinity of the left boundary but grows as the flow of particles propagates to the right hand side of domain $\mathcal{D}$. This is all the more emphasized by the realisations of $U^P(x,t)$ on the same pictures: for the three earliest times $t = 0.1, 0.5, 1.0$, the front of the particle propagation has a zero variance. The positive variance is only in the wake of the particle flow. After the reshock on the right boundary, the whole domain is affected by a positive variance. The right column of figure 3 presents the variance of U^P for $P \in \{2,...,7\}$ for the same times. Once again, for early times, the convergence is fast: $P \in \{3,...,7\}$ gives almost the same results, only the solution obtained from the $P = 2$-truncated reduced model presents a coarse behaviour at this time. As time increases, the differences between the several reduced model results become more and more visible. At time $t = 2.0$, the need for higher truncation orders P is visible. On this same picture, the fast convergence is noticeable, even without having access to an analytical solution, as the gaps between the solutions obtained with P and $P+1$ are decreasing quickly with P.

Remark 4.1 *Note that this test-case, with uncertainties affecting the angular scattering, has been introduced to be able to observe a gain with respect to increasing orders P: in the test-cases of [47], the convergence is so fast that all truncation orders are converged for small values of P.*

5 Conclusion and open problems

In this paper, we considered the linear Boltzmann equation subject to uncertainties in the initial conditions and model parameters. In order to solve the underlying uncertain problem, we relied on moment theory and the construction of gPC based reduced models. The main result of this paper is the proof of the spectral convergence of the gPC based reduced models of the uncertain linear Boltzmann equation. The long-term behaviour of gPC reduced models have been theoretically put forward. The

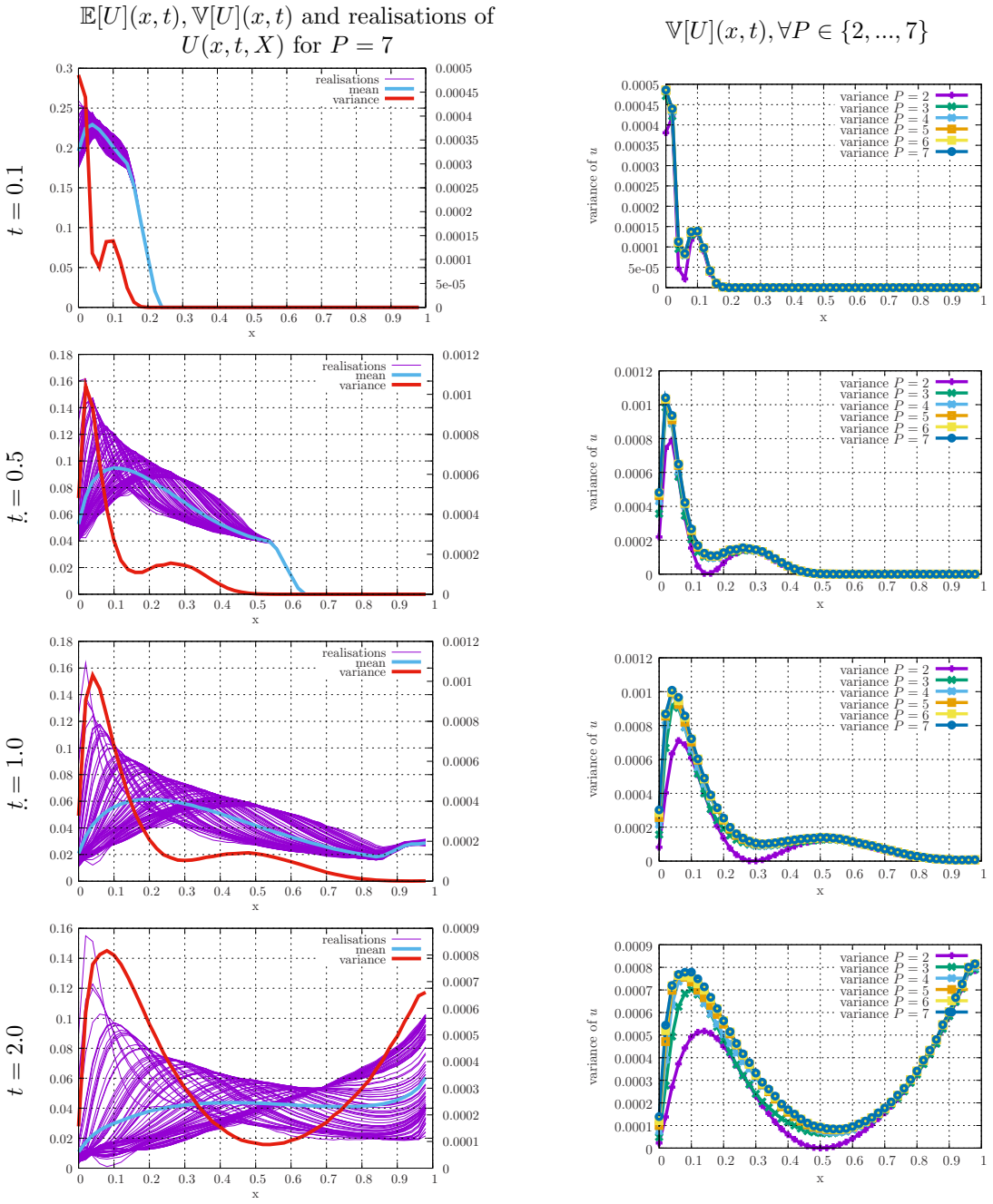

Figure 3: All the results of this figure have been obtained applying the gPC-i-MC scheme of [47]. Left: time evolution of the mean and variance profiles together with 200 realisations recovered thanks to the use of $P = 7$-truncated gPC reduced model. Right: convergence studies on the variance of U with respect to P in the same condition as for the left column (time evolution of the profiles of the variance for $P \in \{2, ..., 7\}$.

fast convergence of the approximations has also been recovered numerically. The numerical test-problems have been built to allow emphasizing the limitations of the theoretical result proved in this paper: some bounds are probably not optimal and theorem 1 may be pessimistic, especially for

absorbing media. Still, this is encouraging as it implies the numerical convergence is even faster than the expected one.

We finally would like to finish on few questions related to the ones discussed in this paper which we think may be of importance: first, despite the fast convergence rate of the reduced models, no positivity results on the uncertain density of particles is ensured. In practice, we did not encounter any problems as our computations are accurate enough and the robustness of our algorithm, see [47], does not rely on such condition. But this does not ensure positivity in future computations and may be problematic for some applications. The second problem is the curse of dimensionality and the fact the bigger the dimension Q of the uncertain vector X, the more coefficients are to be estimated. This point is addressed in [47]: the curse of dimensionality is partly compensated by an astute use of a Monte-Carlo scheme (less sensitive to the dimension) together with the ingredient of this paper. The last point we suggest to tackle is closely related to remark 3.1. There is a lack of theory for non uniform input random variables with respect to spectral convergence. In practice, spectral convergence is observed in many physical domains with respect to any input distribution. But the problem of having polynomials on unbounded domains (typically, we can not use a majoration such as (23) on an unbounded domain) makes the understanding more complex. Still, some results exists for L^∞ bounds in weighted spaces [37] and future effort will probably be carried on in this direction.

References

[1] Brunner T. A. and P. S. Brantley. An efficient, robust, domain-decomposition algorithm for particle Monte Carlo. *Journal of Computational Physics*, 228.10:3882–3890, 2009.

[2] Milton Abramowitz and Irene A. Stegun. *Handbook of Mathematical Functions with Formulas, Graphs, and Mathematical Tables*. Dover, New York, ninth dover printing, tenth gpo printing edition, 1964.

[3] R. Dautray annd J.L. Lions. *Analyse mathématique et calcul numérique pour les sciences et les techniques*, volume tome 1-6. Masson, 1984.

[4] G. Blatman. *Adaptive sparse polynomial chaos expansions for uncertainty propagation and sensitivity analysis*. Thèse de doctorat, Université Blaise Pascal - Clermont II, 2009.

[5] G. Blatman and B. Sudret. Sparse Polynomial Chaos Expansions and Adaptive Stochastic Finite Elements using a Regression Approach. *C. R. Méc.*, 336:518–523, 2008.

[6] G. Blatman and B. Sudret. Efficient computation of global sensitivity indices using sparse polynomial chaos expansions. *Rel. Eng. Syst. Saf.*, 95:1216–1229, 2010.

[7] G. Blatman, B. Sudret, and M. Berveiller. Quasi-Random Numbers in Stochastic Finite Element Analysis. *Mech. Ind. proofs*, 8:289–297, 2007.

[8] Emeric Brun, Stéphane Chauveau, and Fausto Malvagi. Patmos: A prototype monte carlo transport code to test high performance architectures. In Proceedings of International Conference on Mathematics & Computational Methods Applied to Nuclear Science & Engineering, Jeju, Korea, 2017.

[9] Cacucci and Dan G. *Handbook of Nuclear Engineering*, volume 1. Springer Science & Business Media, 2010.

[10] R.H. Cameron and W.T. Martin. The Orthogonal Development of Non-Linear Functionals in Series of Fourier-Hermite Functionals. *Annals of Math.*, 48:385–392, 1947.

[11] Jose Antonio Carrillo and Mattia Zanella. Monte Carlo gPC methods for diffusive kinetic flocking models with uncertainties. 2019. preprint.

[12] T. Crestaux. Polynômes de Chaos pour la Propagation et la Quantification d'Incertitudes. Technical report, CEA, 2006.

[13] M. K. Deb, I. M. Babuska, and J. T. Oden. Solution of Stochastic Partial Differential Equations using Galerkin Finite Element Techniques. *Comp. Meth. Appl. Mech. Engrg.*, 190:6359–6372, 2001.

[14] Bruno Després, Gaël Poëtte, and Didier Lucor. *Robust Uncertainty Propagation in Systems of Conservation Laws with the Entropy Closure Method*, volume 92 of *Lecture Notes in Computational Science and Engineering*. Uncertainty Quantification in Computational Fluid Dynamics, 2013.

[15] J. Dufek and W. Gudowski. Stochastic approximation for Monte-Carlo Calculation of Steady-State Conditions in Thermal Reactors. *Nucl. Sci. Ener.*, 152:274–283, 2006.

[16] Jakob Dürrwächter, Thomas Kuhn, Fabian Meyer, Louisa Schlachter, and Florian Schneider. A hyperbolicity-preserving discontinuous stochastic galerkin scheme for uncertain hyperbolic systems of equations. arXiv:1805.10177.

[17] Ernst, Oliver G., Mugler, Antje, Starkloff, Hans-Jörg, and Ullmann, Elisabeth. On the convergence of generalized polynomial chaos expansions. *ESAIM: M2AN*, 46(2):317–339, 2012.

[18] P. Frauenfelder, C. Schwab, and R.A. Todor. Finite Element for Elliptic Problems with Stochastic Coefficients. *Comp. Meth. Appl. Mech. Engrg.*, 194:205–228, 2004.

[19] Walter Gautschi. *Orthogonal polynomials: applications and computation*, volume 5. Oxford University Press, 1996.

[20] M. I. Gerritsma, J.-B. van der Steen, P. Vos, and G. E. Karniadakis. Time-dependent generalized polynomial chaos. *J. Comput. Physics*, pages 8333–8363, 2010.

[21] R. G. Ghanem and J. Red-Horse. Propagation of Uncertainty in Complex Physical Systems using a Stochastic Finite Elements Approach. *Physica D*, 133:137–144, 1999.

[22] R.G. Ghanem. Ingredients for a General Purpose Stochastic Finite Element Formulation. *Comp. Meth. Appl. Mech. Eng.*, 168:19–34, 1999.

[23] R.G. Ghanem and P. Spanos. *Stochastic Finite Elements: a Spectral Approach*. Springer-Verlag, 1991.

[24] R.G. Ghanem and P.D. Spanos. *Stochastic Finite Elements: a Spectral Approach*. Dover, 1991.

[25] F. Golse and G. Allaire. *Transport et Diffusion*. 2015. Polycopié de cours.

[26] Bal Guillaume. *Couplage d'equations et homogeneisation en transport neutronique*. PhD thesis, Université Paris 6, France, 1997.

[27] T.D. Hien and M. Kleiber. Stochastic Finite Element Modeling in Linear Transient Heat Transfer. *Comp. Meth. Appl. Mech. Engrg.*, 144:111–124, 1997.

[28] M. Jardak, C.H. Su, and G.E. Karniadakis. Spectral polynomial chaos solutions of the stochastic advection equation. *Journal of Scientific Computing*, 17(1):319–338, 2002.

[29] A. Keese. *A General Purpose Framework for Stochastic Finite Elements*. Ph. d. thesis, Mathematik und Informatik der Technischen Universitat Braunschweig, 2004.

[30] J. Kusch, G. W. Alldredge, and M. Frank. Maximum-principle-satisfying second-order intrusive poly- nomial moment scheme. *arXiv preprint arXiv:1712.06966*, 2017.

[31] J. Kusch and M. Frank. Intrusive methods in uncertainty quantification and their connection to kinetic theory. *International Journal of Advances in Engineering Sciences and Applied Mathematics*, pages 1–16, 2018.

[32] Jonas Kusch, Ryan G. McClarren, and Martin Frank. Filtered stochastic galerkin methods for hyperbolic equations. *J. Comput. Phys.*, 2018.

[33] B. Lapeyre, E. Pardoux, and R. Sentis. *Méthodes de Monte Carlo pour les équations de transport et de diffusion*. Number 29 in Mathématiques & Applications. Springer-Verlag, 1998.

[34] O. Le Maitre, M. Reagan, H. Najm, R. Ghanem, and O. Knio. Multi-Resolution Analysis of Wiener-Type Uncertainty Propagation Schemes. *J. Comp. Phys.*, 197:502–531, 2004.

[35] R. Lebrun and A. Dutfoy. A Generalization of the Nataf Transformation to Distributions with Elliptical Copula. *Prob. Eng. Mech.*, 24,2:172–178, 2009.

[36] R. Lebrun and A. Dutfoy. An Innovating Analysis of the Nataf Transformation from the Copula viewpoint. *Prob. Eng. Mech.*, 24,3:312–320, 2009.

[37] A.L. Levin and D.S. Lubinsky. Bounds for orthogonal polynomials for exponential weights. *Journal of Computational and Applied Mathematics*, 99(1):475 – 490, 1998. Proceeding of the VIIIth Symposium on Orthogonal Polynomials and Thier Application.

[38] E. E. Lewis and W. F. Miller Jr. *Computational Methods of Neutron Transport*. John Wiley and Son New York, 1984.

[39] O. P. Le Maître and O. M. Knio. Uncertainty Propagation using Wiener-Haar Expansions. *J. Comp. Phys.*, 197:28–57, 2004.

[40] O. P. Le Maître and O. M. Knio. A Stochastic Particle-Mesh Scheme for Uncertainty Propagation in Vortical Flows. *J. Comp. Phys.*, 226:645–671, 2007.

[41] et al Martin, William R. Monte carlo photon transport on shared memory and distributed memory parallel processors. *International Journal of High Performance Computing Applications*, 1.3:57–74, 1987.

[42] L. Mathelin and O. P. Le Maître. A Posteriori Error Analysis for Stochastic Finite Element Solutions of Fluid Flows with Parametric Uncertainties. *ECCOMAS CFD*, 2006.

[43] J. Mercer. Functions of Positive and Negative Type and their Connection with the Theory of Integral Equations. *Philos. Trans. Roy. Soc.*, 209, 1909.

[44] M. Meyer and H.G. Matthies. Efficient model reduction in non-linear dynamics using the Karhunen-Loève expansion and dual-weighted-residual methods. *Comp. Meth. Appl. Mech. Eng.*, Informatikbericht 2003-08, TU Braunschweig, Germany, 2004.

[45] H. N. Najm O.P. Le Maître, O. M. Knio and R. G. Ghanem. A Stochastic Projection Method for Fluid Flow I: Basic Formulation. *J. Comp. Phys.*, 173:481–511, 2001.

[46] G. C. Papanicolaou. Asymptotic Analysis of Transport Processes. *Bulletin of the American Mathematical Society*, 81(2), 1975.

[47] Gaël Poëtte. A gPC-intrusive Monte-Carlo scheme for the resolution of the uncertain linear Boltzmann equation. *Journal of Computational Physics*, 385:135 – 162, 2019.

[48] J. Spanier and E. M. Gelbard. *Monte Carlo Principles and Neutron Transport Problems*. Addison-Wesley, 1969.

[49] P. Spanos and R. G. Ghanem. Stochastic Finite Element Expansion for Random Media. *ASCE J. Eng. Mech.*, 115(5):1035–1053, 1989.

[50] B. Sudret and A. Der Kiureghian. Stochastic Finite Element Methods and Reliability - A State of the Art Report. Technical Report UCB/SEMM-2000/08, Department of civil and environmental engineering, University of California, Berkeley, 2000.

[51] R. A. Todor and C. Schwab. Karhunen-Loève approximation of random fields by generalized fast multipole methods. *J. Comp. Phys.*, 217(1):100–122, 2006.

[52] J. Tryoen, O. Le Maître, and A. Ern. Adaptive Anisotropic Stochastic Discretization Schemes for Uncertain Conservation Laws. *Proc. of ASME 2010, Third Joint US-European Fluids Engineering Summer Meeting*, 2010.

[53] P. Vos. Time dependent polynomial chaos. Master of science thesis, Delft University of technology, Faculty of Aerospace engineering, 2006.

[54] X. Wan and G.E. Karniadakis. Beyond Wiener-Askey Expansions: Handling Arbitrary PDFs. *SIAM J. Sci. Comp.*, 27(1-3), 2006.

[55] X. Wan and G.E. Karniadakis. Long-Term Behavior of Polynomial Chaos in Stochastic Flow Simulations. *Comp. Meth. Appl. Mech. Engng*, 195:5582–5596, 2006.

[56] X. Wan and G.E. Karniadakis. Multi-Element generalized Polynomial Chaos for Arbitrary Probability Measures. *SIAM J. Sci. Comp.*, 28(3):901–928, 2006.

[57] N. Wiener. The Homogeneous Chaos. *Amer. J. Math.*, 60:897–936, 1938.

[58] J. A. S. Witteveen and H. Bijl. An Unsteady Adaptive Stochastic Finite Elements Formulation for Rigid-Body Fluid-Structure Interaction. *Comp. and Struct.*, 2008.

[59] D. Xiu and G.E. Karniadakis. Modeling Uncertainty in Steady State Diffusion Problems via generalized Polynomial Chaos. *Comp. Meth. Appl. Mech. Engrg.*, 191:4927–4948, 2002.

[60] D. Xiu and G.E. Karniadakis. Modeling Uncertainty in Flow Simulations via generalized Polynomial Chaos. *Comp. Meth. Appl. Mech. Engrg.*, 187:137–167, 2003.